Quantifying the effects of strength- and speed-like interventions on epidemic dynamics

Sang Woo Park[1,*], Kaiyuan Sun, Benjamin M. Bolker, Bryan T. Grenfell, Jonathan Dushoff, [**SWP:** *and others if needed*]

1 Department of Ecology and Evolutionary Biology, Princeton University, Princeton, NJ, USA

*Corresponding author: swp2@princeton.edu

1 Introduction

The reproduction number $\mathcal{R}$—typically defined as the average number of new infections caused by an infected individual—is a key characteristic of an emerging epidemic. Its value in a fully susceptible population—the *basic* reproduction number, $\mathcal{R}_0$—provides information about whether a pathogen can invade, the level of intervention required to prevent invasion, and the final size of an epidemic (Diekmann et al., 1990; Anderson and May, 1991). When an epidemic is ongoing, transmission dynamics are affected by changes in population-level immunity, non-pharmaceutical interventions, and contact patterns—these changes in transmission dynamics can be described by $\mathcal{R}(t)$, often referred to as the *effective* or *time-dependent* reproduction number (Wallinga and Teunis, 2004; Fraser, 2007; Cori et al., 2013). Interpretation and estimation of $\mathcal{R}(t)$ have been a key area of research during the ongoing COVID-19 outbreaks due to its policy implications (Pan et al., 2020; Flaxman et al., 2020; Gostic et al., 2020).

One of the main challenges in interpreting $\mathcal{R}(t)$ can be attributed, in part, to its standard, heuristic definition: the average number of new infections caused by an infected individual. While this definition is biologically intuitive, it is mathematically imprecise as time-dependent reproduction numbers can be defined in multiple ways, depending on the cohort (e.g., a group of individuals who developed symptoms or were infected at the same time) and the types of transmission scenarios (i.e., realized or counterfactual transmission processes). Here, we primarily focus on two main measures of transmission that look at a cohort of infectees or infectors that were infected at the same time: the instantaneous reproduction number $\mathcal{R}_\mathrm{i}(t)$ and the case reproduction number $\mathcal{R}_\mathrm{c}(t)$.

The instantaneous reproduction number $\mathcal{R}_\mathrm{i}(t)$—popularized by Cori et al. (2013)—was initially defined as the "average number of people someone infected at time t could expect to infect should conditions remain unchanged" (Fraser, 2007). While this definition is correct, we note that there are additional subtleties to defining $\mathcal{R}_\mathrm{i}(t)$. In fact, $\mathcal{R}_\mathrm{i}(t)$ does not actually depend on when the person gets infected, only on when the conditions are held constant at: if we freeze conditions at time t, anyone who become infected after time t will cause same number of infections on average. But transmission conditions always change over the course of an epidemic due to the susceptible depletion and other behavioral effects, meaning that

$\mathcal{R}_{\mathrm{i}}(t)$ is a counterfactual quantity. Nonetheless, we care about $\mathcal{R}_{\mathrm{i}}(t)$ because it characterizes transmission conditions at time t and therefore provides a real-time estimate of whether the disease will continue to spread if conditions were to stay the same (Gostic et al., 2020).

The case reproduction number $\mathcal{R}_{\mathrm{c}}(t)$—popularized by Wallinga and Teunis (2004)—corresponds to the average number of new infections that an individual infected at time t generated over the course of their infection. $\mathcal{R}_{\mathrm{c}}(t)$ is a realized measure, which depends on conditions after time t and can only be estimated retrospectively. Although the heuristic definition of $\mathcal{R}(t)$ ("the average number of new infections caused by an infected individual") closely resembles that of $\mathcal{R}_{\mathrm{c}}(t)$, the mathematical definitions of $\mathcal{R}(t)$ derived from standard compartmental models (e.g., basic reproduction multiplied by the proportion susceptible) actually correspond to that of $\mathcal{R}_{\mathrm{i}}(t)$ (Gostic et al., 2020). Hereafter, we use $\mathcal{R}(t)$ to refer to the instantaneous reproduction number $\mathcal{R}_{\mathrm{i}}(t)$ and return to the distinction between $\mathcal{R}_{\mathrm{i}}(t)$ and $\mathcal{R}_{\mathrm{c}}(t)$ later.

Analogous to the reproduction number $\mathcal{R}$, exponential growth rate r describes the speed at which infection spreads at the population level. When conditions remain the same, both $\mathcal{R}$ and r provide equivalent threshold measures for control and are linked by the generation-interval distribution $g(\tau)$, where generation intervals describe time between infections of an infector and an infectee (Svensson, 2007). Throuhgout the pandemic, most analyses relied on changes in $\mathcal{R}(t)$ to evaluate the impact of intervention (Flaxman et al., 2020; Brauner et al., 2021). A few studies have adopted time-varying growth rates $r(t)$ to monitor the spread of infections, but there has been a limited understanding of the relationship between $\mathcal{R}(t)$ and $r(t)$. For example, Parag, Thompson, and Donnelly (Parag et al.) argued that $\mathcal{R}(t)$ is theoretically more informative than $r(t)$ when the generation-interval distribution is known and underlying assumptions about pathogen transmission hold. However, they are better seen as complementary measures, with the relative value dependent on what information is available and what interventions are being considered (Dushoff and Park, 2021).

In this study, we extend the strength–speed framework by Dushoff and Park (2021) to iillustrate the differences between $\mathcal{R}(t)$ and $r(t)$ in characterizing changes in epidemic dynamics. Here, epidemic "strength" and "speed" refers to the reproduction number $\mathcal{R}$ and the growth rate r, respectively; in parallel, we use "constant-strength" and "constant-speed" interventions to refer to idealized interventions that directly affect $\mathcal{R}$ and r, respectively. For example, a constant-strength intervention that reduces the transmission rate by a constant amount θ throughout infection can control the epidemic when $\theta > \mathcal{R}$. Analogously, a constant-speed intervention that isolates infected individuals at a constant rate ϕ throughout infection can control the epidemic when $\phi > r$. We note that these idealized interventions are constant across time of infection, but not across calendar time—in other words, constant-strength and -speed interventions of varying effectiveness can be introduced and lifted throughout an epidemic.

In extending the strength–speed framework, we begin by showing that the renewal process of infection can be expressed in two equivalent ways using instantaneous and case-based perspectives. The first renewal equation relies on the instantaneous reproduction number $\mathcal{R}_{\mathrm{i}}(t)$, and therefore connects past and current incidence using a counterfactual distribution, which corresponds to the instantaneous generation-interval distribution. The second renewal

equation relies on the case reproduction number $\mathcal{R}_c(t)$, a realized measure of transmission, and therefore connects past and current incidence using a realized distribution, which we call the forward generation-interval distribution. Instantaneous and forward generation-interval distributions differ qualitatively in the way they change through time. For example, a constant-strength intervention causes the forward distribution to change over time even though the instantaneous distribution remains invariant. On the other hand, a constant-speed intervention causes both distributions to change, which must be taken into account to correctly estimate $\mathcal{R}_i(t)$ and $\mathcal{R}_c(t)$. Instead, the time-varying growth rate $r(t)$ is a robust measure for changes in incidence under both constant-strength and constant-speed interventions as it does not require assumptions about the underlying distribution. Finally, we link a simple SIR model with the renewal equation framework to show that changes in the transmission rate are equivalent to a constant-strength intervention, whereas changes in the recovery rate are equivalent to a constant-speed intervention—we thus conclude that $\mathcal{R}(t)$ is generally a better measure for characterizing disease spread under constant-strength interventions, whereas $r(t)$ is generally better under constant-speed interventions.

2 Mathematical theory

2.1 Renewal equation framework

The renewal equation framework provides a flexible way of modeling the spread of infection and the impact of intervention (Fraser, 2007). Let $K(t,\tau)$ represent the infection kernel, defined as the rate at which secondary cases are generated at time t by an individual infected τ time units ago (we will use s,t to denote calendar time and σ,τ to denote time since infection throughout). The shape of this kernel can depend on characteristics of the infection (e.g., variation in infectiousness over the course of infection) as well as other population-level factors (e.g., susceptible depletion, non-pharmaceutical interventions, and changes in behavior). Then, incidence of infection at time t caused by a cohort of individuals infected τ time units ago can be written as the product of the kernel, $K(t,\tau)$, and incidence at time $t-\tau$, $i(t-\tau)$:

$$i_{t-\tau}(t) = K(t,\tau)i(t-\tau). \tag{1}$$

Integrating across time since infection τ allows us to express the dynamics of incidence $i(t)$ using a renewal-equation framework:

$$i(t) = \int_0^\infty K(t,\sigma)i(t-\sigma)\,\mathrm{d}\sigma. \tag{2}$$

This formulation generalizes the dynamics of many compartmental models, including the standard SEIR model (Heesterbeek and Dietz, 1996; Diekmann and Heesterbeek, 2000; Roberts, 2004; Aldis and Roberts, 2005; Roberts and Heesterbeek, 2007; Champredon et al., 2018).

Here, we show that the dynamics of this infection model can be expressed equivalently in terms of instantaneous quantities or in terms of realized quantities, meaning $\mathcal{R}_i(t)$ and

$\mathcal{R}_c(t)$ with their corresponding generation-interval distributions. The integral of $K(t,\tau)$ across τ with t fixed gives the instantaneous reproduction number (Fraser, 2007): $\mathcal{R}_i(t) = \int K(t,\sigma)\,\mathrm{d}\sigma$. If we normalize this kernel, we get the instantaneous generation-interval distribution $g_t(\tau) = K(t,\tau)/\mathcal{R}_i(t)$. The instantaneous reproduction number and generation-interval distribution describe (counterfactual) quantities that would be realized only if conditions remained constant (i.e., if $K(s,\tau) = K(t,\tau)$ for all $s \geq t$). The renewal equation (Eq. 2) can be rewritten using this decomposition:

$$i(t) = \mathcal{R}_i(t) \int_0^\infty g_t(\sigma) i(t-\sigma)\,\mathrm{d}\sigma. \tag{3}$$

For example, if disease parameters remain constant in a simple model, such as the SEIR model, we would expect $\mathcal{R}_i(t) = \mathcal{R}_0 S(t)$ and $g_t(\tau) = g_0(\tau)$, where $g_0(\tau)$ represents the intrinsic generation-interval distribution (Champredon and Dushoff, 2015).

Now, consider the forward kernel $F_t(\tau)$, which represents the rate at which an individual infected at time t generates secondary infections τ time units after infection:

$$F_t(\tau) = K(t+\tau,\tau). \tag{4}$$

The integral of $F_t(\tau)$, representing the total infectiousness of an individual infected at time t, corresponds to the case reproduction number: $\mathcal{R}_c(t) = \int F_t(\sigma)\,\mathrm{d}\sigma$. The forward kernel, normalized by the total infectiousness, corresponds to the forward generation-interval distribution $f_t(\tau) = F_t(\tau)/\mathcal{R}_c(t)$, describing realized generation intervals for a cohort of infectors that were infected at time t. Then, the forward renewal equation can be written as:

$$i(t) = \int_0^\infty \mathcal{R}_c(t-\sigma) f_{t-\sigma}(\sigma) i(t-\sigma)\,\mathrm{d}\sigma. \tag{5}$$

This forward renewal equation provides an equivalent description of the infection processes as the instantaneous form (Eq. 3).

We can check that the instantaneous quantities ($\mathcal{R}_i(t)$ and $g_t(\tau)$) match the forward realized quantities ($\mathcal{R}_c(t)$ and $f_t(\tau)$) when conditions remain constant (or effectively constant, as in the case of early exponential spread). Assuming that $K_s(\tau) = K_t(\tau)$ for all $s \geq t$, we obtain $F_t(\tau) = K(t,\tau)$ (and therefore, $\mathcal{R}_c(t) = \mathcal{R}_i(t)$ and $f_t(\tau) = g_t(\tau)$).

2.2 Constant-strength and constant-speed interventions

To model changes in epidemic dynamics, we introduce an intervention function $\mathcal{I}(t,\tau)$ which can depend on both calendar time t as well as time since infection τ. Then, the infection kernel under $\mathcal{I}$ at calendar time t can be written as:

$$K(t,\tau) = \mathcal{R}_0 \mathcal{I}(t,\tau) g_0(\tau), \tag{6}$$

where g_0 is the pre-intervention instantaneous generation interval (assumed to remain nearly constant for the time period of interest, apart from the effects of the intervention) The forward kernel of an individual infected at time t under $\mathcal{I}$ can then be written as:

$$F_t(\tau) = \mathcal{R}_0 \mathcal{I}(t+\tau,\tau) g_0(\tau). \tag{7}$$

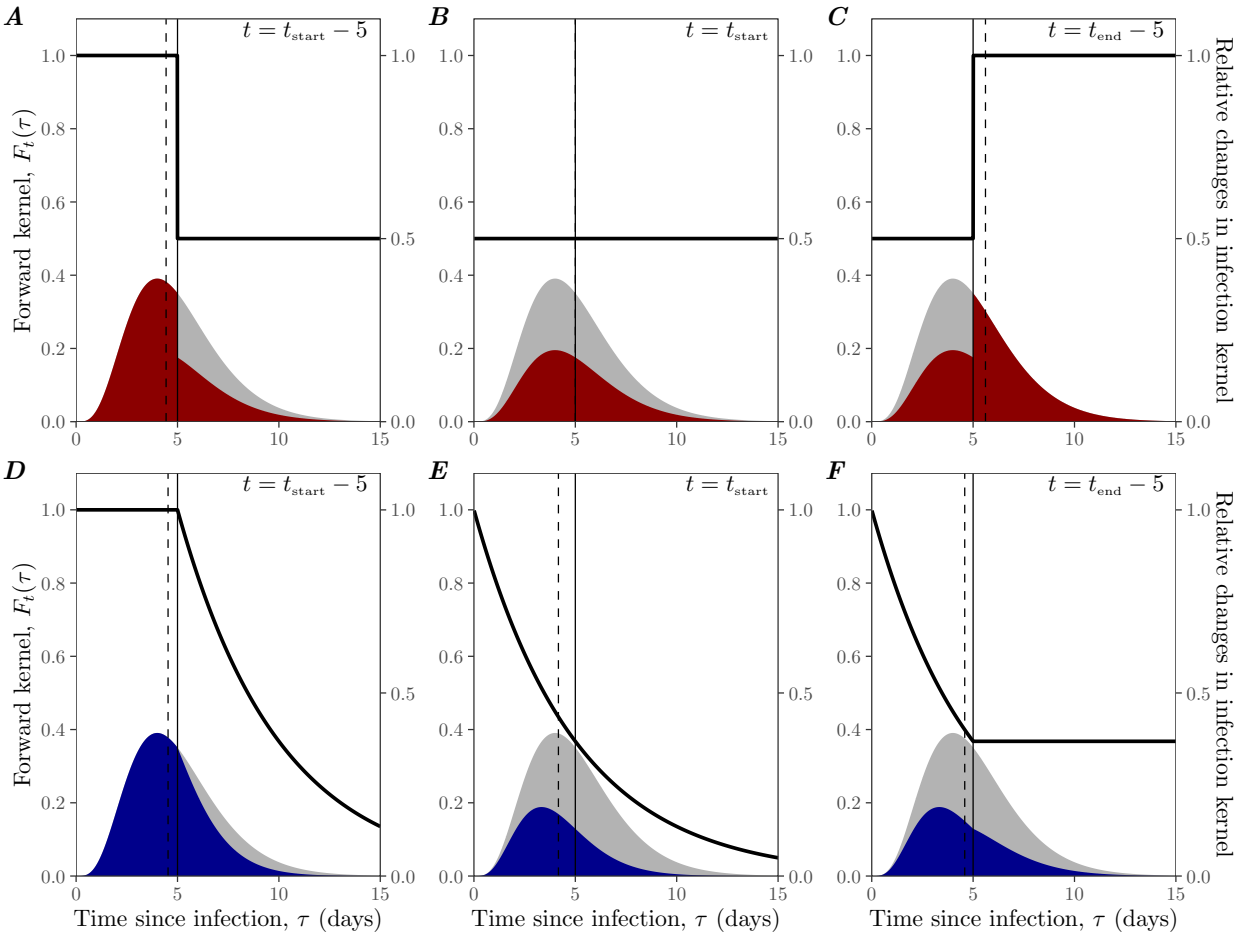

Figure 1: **The impact of constant-strength and constant-speed interventions on forward kernels.** The impact of constant-strength (A–C) and constant-speed (D–F) intervention on forward kernels of cohort of individuals infected at different time: 5 days before intervention onset (A, D), during intervention (B, E), and 5 days before intervention offset (C, F). Gray shaded curves represent the (fixed) intrinsic kernel $K_0(\tau)$, which is modeled using a gamma distribution with $\mathcal{R}_0$ of 2, a mean of 5 days and a squared coefficient of variation of 0.2. Colored curves represent the forward kernel $F_t(\tau)$ under strength-based (A–C) and speed-based (D–F) interventions. The strength-based intervention is assumed to reduce kernel by a factor of 2. The speed-based intervention is assumed to have a constant hazard of 1/5/days during the intervention period. Susceptible depletion is assumed to be negligible. Solid black lines represent relative changes in the kernel: $F_t(\tau)/K_0(\tau)$. Solid vertical lines show the (fixed) mean intrinsic generation interval and dashed vertical lines the mean forward generation interval.

The intervention function $\mathcal{I}(t, \tau)$ can capture any kinds of epidemiological changes, including changes in the susceptible pools $S(t)$ (either due to natural infection or vaccination) as well as introduction and lifting of non-pharmaceutical interventions.

We focus on two idealized interventions, which we refer to as constant-strength and constant-speed interventions, and later generalize them (Dushoff and Park, 2021). While our primary focus is on the instantaneous quantities ($\mathcal{R}_{\mathrm{i}}(t)$ and $g_t(\tau)$), we first illustrate the impact of constant-strength and constant-speed interventions using forward quantities as they describe realized transmission processes and are easier to interpret.

First, we consider a constant-strength intervention $\mathcal{I}(t,\tau) = \mathcal{P}(t)$, which reduces the transmission rate by a constant amount across the age of infection τ at a given time t; note that $\mathcal{P}(t)$ need not be constant across calendar time. For example, a constant-strength intervention that reduces transmission by a factor of ϕ between time t_{start} and t_{end} can be modeled as:

$$\mathcal{P}(t) = \begin{cases} 1 & t < t_{\mathrm{start}} \\ \frac{1}{\phi} & t_{\mathrm{start}} \leq t < t_{\mathrm{end}} \\ 1 & t_{\mathrm{end}} \leq t \end{cases}. \tag{8}$$

Fig. 1A–C illustrates the impact of such intervention on the forward kernel $F_t(\tau)$ of an individual infected 5 days before t_{start}, at t_{start}, and 5 days before t_{end}. This constant-strength intervention reduces transmission immediately (Fig. 1A); likewise, lifting this intervention can, in theory, can cause the forward kernel to return back to normal immediately (Fig. 1C). Even though the exact shape of the kernel $F_t(\tau)$ depends on the time of infection and when the intervention was introduced relative to the infection time, the relative impact of intervention in reducing transmission (black solid lines in Fig. 1A–C, representing $F_t(\tau)/K(0,\tau)$) is constant ($1/\phi$) for transmission that occurs during the intervention period.

Such intervention has predictable effects on mean generation intervals: implementing (lifting) intervention decreases (increases) future transmission potential and therefore decreases (increases) the mean forward generation interval (Fig. 1A,C). If an individual is infected after t_{start} (and much earlier than t_{end}), this intervention simply reduces the entire kernel by a constant amount and has no effect on realized generation intervals (Fig. 1B). This observation generalizes the phenomenon of contraction of realized generation intervals due to susceptible depletion (Kenah et al., 2008; Nishiura, 2010; Champredon and Dushoff, 2015).

Analogously, we consider a constant-speed intervention $\mathcal{I}(t,\tau) = \mathcal{H}(t,\tau)$ that depends on time-varying hazard of isolation $h(t)$:

$$\mathcal{H}(t,\tau) = \exp\left(-\int_0^\tau h(t-\sigma)\,\mathrm{d}\sigma\right). \tag{9}$$

Analogous to the constant-strength intervention, the constant-speed intervention assumes a constant hazard of isolation across the age of infection τ at a given time t; however, the hazard need not be constant across calendar time. Then, $\mathcal{H}(t,\tau)$ represents the probability that an individual infected τ time units ago has not been isolated by calendar time t. In practice, the hazard of isolation is expected to depend not only on calendar time t but also on the age of infection τ—for example, we expect $h(t,\tau)$ to increase with τ for symptom-based interventions to reflect the increasing cumulative probability of developing symptoms.

For example, a constant-speed intervention that takes place between time t_{start} and t_{end} can be modeled using the following hazard function:

$$h(t) = \begin{cases} 0 & t < t_{\text{start}} \\ \theta & t_{\text{start}} \leq t < t_{\text{end}} \\ 0 & t_{\text{end}} \leq t \end{cases}. \tag{10}$$

In this case, the probability that an individual infected at time t has not been isolated by τ time units after infection depends on the amount of time the individual has been exposed to this intervention. If the individual is infected before t_{start}, they will not be isolated by this intervention until after t_{start}. If the individual is infected after t_{end}, they will never be isolated by this intervention. Fig. 1D–E illustrates the impact of such intervention on the forward kernel of an individual infected 5 days before t_{start}, at t_{start}, and 5 days before t_{end}. Unlike the constant-strength intervention, the constant-speed intervention does not show effects immediately; that is, the rate at which an infected individual generates secondary infections at time t_{start} remains unaffected by the intervention because it takes time to identify and isolate infected individuals. On the other hand, when the intervention is lifted at t_{end}, the value of the kernel at calendar time remains unchanged because some fraction of infected individuals have already been isolated. The constant-speed interventions always shorten realized generation intervals because they prevent late transmission (Fig. 1D–E).

Finally, we can decompose the generalized intervention function $\mathcal{I}(t,\tau)$ as a product of constant-strength and constant-speed interventions: $\mathcal{I}(t,\tau) = \mathcal{P}(t)\mathcal{H}(t,\tau)$. Then, the dynamics of incidence $i(t)$ can be written as:

$$i(t) = \mathcal{R}_0 \mathcal{P}(t) \int_0^\infty \mathcal{H}(t,\sigma) g_0(\sigma) i(t-\sigma)\, \mathrm{d}\sigma. \tag{11}$$

In this case, the instantaneous reproduction number and generation-interval distributions are given by:

$$\mathcal{R}_{\text{i}}(t) = \mathcal{R}_0 \mathcal{P}(t) \int_0^\infty \mathcal{H}(t,\sigma) g_0(\sigma)\, \mathrm{d}\sigma, \tag{12}$$

$$g_t(\tau) = \frac{\mathcal{H}(t,\tau) g_0(\tau)}{\int_0^\infty \mathcal{H}(t,\sigma) g_0(\sigma)\, \mathrm{d}\sigma}, \tag{13}$$

which allow us to express the renewal equation in the form of Eq. 3. Therefore, the instantaneous generation-interval distribution changes under constant-speed interventions but not under constant-strength interventions, even though both types of interventions affect the realized generation-interval distribution.

2.3 Quantifying changes in generation-interval distributions

In order to model the renewal process, we have to know how the instantaneous generation-interval distribution $g_t(\tau)$ changes across time t. The instantaneous distribution measures the

infectiousness of an individual infected τ time units ago at time t and is therefore different from the distribution of realized generation intervals (i.e., time between actual infection events). For example, while both the forward generation-interval distribution $f_{t-\tau}(\tau)$ and the instantaneous generation-interval distribution $g_t(\tau)$ depend on the rate at which secondary cases at time t are generated by a primary case infected at time $t-\tau$, $K(t,\tau)$, they are normalized by different quantities:

$$f_{t-\tau}(\tau) = \frac{K(t,\tau)}{\int_0^\infty K(t-\tau+\sigma,\sigma)\,\mathrm{d}\sigma} \neq \frac{K(t,\tau)}{\int_0^\infty K(t,\sigma)\,\mathrm{d}\sigma} = g_t(\tau). \tag{14}$$

The forward distribution $f_{t-\tau}(\tau)$ is normalized by the average number of new infections caused by an individual infected at time $t-\tau$ (i.e., the case reproduction number, $\mathcal{R}_\mathrm{c}(t-\tau)$). On the other hand, the instantaneous distribution $g_t(\tau)$ is normalized by a counterfactual measure of transmission $\mathcal{R}_\mathrm{i}(t)$.

Rewriting Eq. 4 provides further insight into their differences:

$$f_t(\tau) = \frac{\mathcal{R}_\mathrm{i}(t+\tau)g_t(\tau,\tau)}{\int \mathcal{R}_\mathrm{i}(t+\sigma)g_{t+\sigma}(\sigma)\,\mathrm{d}\sigma}. \tag{15}$$

Even if the instantaneous generation-interval distribution $g_t(\tau)$ remains invariant across time (i.e., $g_t(\tau) = g_0(\tau)$), changes in transmission conditions (therefore, $\mathcal{R}_\mathrm{i}(t)$) are expected to change the shape of the forward generation-interval distribution; for example, as we showed earlier, the instantaneous generation-interval distribution does not change under the constant-strength intervention, but the forward generation-interval distribution changes. Therefore, renewal equation models that rely on the forward form (Eq. 5) but assume time-invariant $f_t(\tau)$ should generally be avoided.

On the other hand, if we were to take all realized generation intervals that end at time t and form a distribution, we obtain what is known as the backward generation-interval distribution, $b_t(\tau)$:

$$b_t(\tau) = \frac{i_{t-\tau}(t)}{\int_0^\infty i_{t-\sigma}(t)\,\mathrm{d}\sigma}. \tag{16}$$

The backward distribution systematically differs from the instantaneous distribution:

$$b_t(\tau) = \frac{g_t(\tau)i(t-\tau)}{\int_0^\infty g_t(\sigma)i(t-\sigma)\,\mathrm{d}\sigma} \tag{17}$$

due to its dependence on previous incidence of infection. For example, when incidence is increasing exponentially, we are more likely to observe shorter generation intervals for a cohort of infectees that were infected at the same time because their infectors are more likely to have been infected recently.

Rewriting Eq. 17 in terms of the forward distribution shows that the backward distribution also depends on the case reproduction number $\mathcal{R}_\mathrm{c}(t-\tau)$ of the cohort of infectors at time $t-\tau$:

$$b_t(\tau) = \frac{\mathcal{R}_\mathrm{c}(t-\tau)f_{t-\tau}(\tau)i(t-\tau)}{\int_0^\infty \mathcal{R}_\mathrm{c}(t-\sigma)f_{t-\sigma}(\sigma)i(t-\sigma)\,\mathrm{d}\sigma}. \tag{18}$$

As defined in Eq. 16, the total density of generation intervals between time $t-\tau$ and time t corresponds to $i_{t-\tau}(t)$ (i.e., the total number of infections at time t caused by a cohort of individuals that were infected at time $t-\tau$), which depends on the incidence $i(t-\tau)$ at time $t-\tau$ as well as their average infectiousness $\mathcal{R}_{\mathrm{c}}(t-\tau)$. In other words, a cohort of infectors that generated more infections will have greater contribution towards the backward generation-interval distribution at a given time. Several studies have noted, in various contexts, that backward distributions of epidemiological delays provide biased estimates of the forward distribution due to effects of this sort (Nishiura, 2010; Champredon and Dushoff, 2015; Park et al., 2020,?).

2.4 Quantifying changes in reproduction numbers

The instantaneous reproduction number $\mathcal{R}_{\mathrm{i}}(t)$ provides a measure for the impact of intervention:

$$\mathcal{R}_{\mathrm{i}}(t) = \int_0^\infty K(t,\sigma)\,\mathrm{d}\sigma, \tag{19}$$

$$= \mathcal{R}_0 S(t)\mathcal{P}(t)\int_0^\infty \mathcal{H}(t,\sigma)g_0(\sigma)\,\mathrm{d}\sigma. \tag{20}$$

Since $\mathcal{R}_{\mathrm{i}}(t)$ measures conditions at time t, one would typically expect to detect changes in $\mathcal{R}_{\mathrm{i}}(t)$ as soon as interventions are implemented—as we see in Eq. 20 (and also in Fig. 1), this is true for changes in a constant-strength intervention $\mathcal{P}(t)$ but not under a constant-speed intervention $\mathcal{H}(t,\sigma)$. Therefore, it has been previously argued that $\mathcal{R}_{\mathrm{i}}(t)$ can provide a real-time measure for whether the disease will continue to spread or not (Gostic et al., 2020).

Estimating $\mathcal{R}_{\mathrm{i}}(t)$ depends on the instantaneous generation-interval distribution $g_t(\tau)$, which can vary across time under constant-speed interventions:

$$g_t(\tau) = \frac{K(t,\tau)}{\mathcal{R}(t)} = \frac{\mathcal{H}(t,\tau)g_0(\tau)}{\int_0^\infty \mathcal{H}(t,\sigma)g_0(\sigma)\,\mathrm{d}\sigma}. \tag{21}$$

By rearranging Eq. 2, we obtain the following estimator for $\mathcal{R}(t)$:

$$\mathcal{R}_{\mathrm{i}}(t) = \frac{i(t)}{\int_0^\infty g_t(\sigma)i(t-\sigma)\,\mathrm{d}\sigma}. \tag{22}$$

While this estimator is similar in form to previously proposed estimators (Fraser, 2007), it differs in allowing for the underlying instantaneous generation-interval distribution to vary across time. In particular, the popular R package `EpiEstim`, Cori et al. (2013) uses the approach while assuming that the underlying instantaneous distribution does not change over time; such methods accurately estimate changes in $\mathcal{R}_{\mathrm{i}}(t)$ under constant-strength interventions, but not necessarily under more general conditions.

When both strength- and speed-like interventions are present during an ongoing epidemic, classical estimators Fraser (2007); Cori et al. (2013) measure a slightly different quantity:

$$\mathcal{R}_{\mathrm{cori}}(t) = \frac{i(t)}{\int_0^\infty g_0(\sigma)i(t-\sigma)\,\mathrm{d}\sigma}. \tag{23}$$

This is the number of infections per infection required to explain current incidence under the counter-factual that the generation-interval distribution has not changed. This estimator is widely used, because it is simple, often robust to estimate, and often a good proxy for $\mathcal{R}_{\mathrm{i}}$. When interventions have speed-like components, however, the exact meaning of this estimator can be difficult to interpret; and it does not necessarily accurately reflect how conditions are changing through time.

The case reproduction number $\mathcal{R}_{\mathrm{c}}(t)$ is similarly complicated. Since $\mathcal{R}_{\mathrm{c}}(t)$ measures the average number of new infections caused by an individual infected at time t, we have

$$\mathcal{R}_{\mathrm{c}}(t) = \frac{\int_0^\infty i_t(t+\sigma)\,\mathrm{d}\sigma}{i(t)}, \tag{24}$$

where $i_t(t+\sigma)$ represents incidence at time $t+\sigma$ caused by individuals who were infected at time t. Substituting Eq. 16, it is straightforward to see that $\mathcal{R}_{\mathrm{c}}(t)$ can be estimated by using the backward generation-interval distribution:

$$\mathcal{R}_{\mathrm{c}}(t) = \frac{\int_0^\infty b_{t+\sigma}(\sigma) i(t+\sigma)\,\mathrm{d}\sigma}{i(t)}. \tag{25}$$

Here, the numerator, which represents the total number of infections caused by individuals infected at time t, is calculated by multiplying future incidence $i(t+\sigma)$ with the probability that future infections are caused by an individual infected at time t $b_{t+\sigma}(\sigma)$. Using Eq. 17, we obtain a Wallinga-Teunis-like estimator (Wallinga and Teunis, 2004):

$$\mathcal{R}_{\mathrm{c}}(t) = \int_0^\infty \left(\frac{g_{t+\sigma}(\sigma) i(t+\sigma)}{\int_0^\infty g_{t+\sigma}(\sigma') i(t+\sigma-\sigma')\,\mathrm{d}\sigma'} \right) \mathrm{d}\sigma. \tag{26}$$

This derivation clarifies that, like the classic estimator for $\mathcal{R}_{\mathrm{i}}$, the classic estimator for $\mathcal{R}_{\mathrm{c}}$ is based on the instantaneous generation-interval distribution, and thus implicitly relies on the assumption that changes in transmission are strength-like and not speed-like.

Some studies have suggested substituting the forward distribution $f_t(\tau)$, including the forward serial-interval distribution, instead to estimate the "time-varying" or the "effective" reproduction number $\mathcal{R}(t)$ (Liu et al., 2018; Ali et al., 2020):

$$\mathcal{R}_{\mathrm{forward}}(t) = \frac{i(t)}{\int_0^\infty i(t-\sigma) f_{t-\sigma}(\sigma)\,\mathrm{d}\sigma}. \tag{27}$$

This choice is potentially problematic, as the forward distribution differs systematically from the instantaneous distribution. For example, under constant-strength interventions, the forward distribution changes over time even though the instantaneous distribution remains time invaraint—these differences can lead to systematic biases. In Section 3, we compare $\mathcal{R}_{\mathrm{forward}}(t)$ with $\mathcal{R}_{\mathrm{i}}(t)$ and $\mathcal{R}_{\mathrm{c}}(t)$.

2.5 Quantifying changes in time-dependent growth rate

The instantaneous reproduction number $\mathcal{R}_{\mathrm{i}}(t)$ provides a long-term threshold for whether the epidemic will *eventually* grow or decline if current conditions remain unchanged; perhaps

counterintuitively, it does not tell us whether the epidemic is growing or not at a given moment. Instead, if we want to quantify whether incidence is increasing or decreasing, we can simply calculate the epidemic growth rate. Researchers often focus on the initial exponential growth rate, but we can look at the per-capita growth rate at any time:

$$r(t) = \frac{1}{i(t)} \frac{\mathrm{d}i(t)}{\mathrm{d}t}. \tag{28}$$

By definition, incidence grows when $r(t) > 0$ (and vice versa)—thus, this provides an instantaneous threshold for incidence of infection (but does not provide information about the long-term behavior).

3 Example: Semi-mechanistic SIR model

In order to understand how constant-strength and constant-speed interventions affect disease spread, we use a semi-mechanistic SIR model to generate synthetic data and compare various estimates of $\mathcal{R}(t)$ and $r(t)$:

$$\frac{\mathrm{d}S}{\mathrm{d}t} = -\beta(t)SI, \tag{29}$$

$$\frac{\mathrm{d}I}{\mathrm{d}t} = \beta(t)SI - \gamma(t)I, \tag{30}$$

$$\frac{\mathrm{d}R}{\mathrm{d}t} = \gamma(t)I, \tag{31}$$

where S, I, R represent proportion of individuals that are susceptible, infected, and removed (either due to recovery or isolation measures); $\beta(t)$ represent time-varying transmission rate; and $\gamma(t)$ represent time-varying removal rate. We refer to this model as semi-mechanistic because the infection and recovery process are modeled explicitly, but changes in β and γ are allowed to change freely over time (without any mechanisms). In this case, the instantaneous kernel can be written as:

$$K(t, \tau) = \beta(t)S(t) \exp\left(-\int_{t-\tau}^{t} \gamma(s)\,\mathrm{d}s\right). \tag{32}$$

We see that changes in transmission rate $\beta(t)$ and removal rate $\gamma(t)$ exactly match the definitions of constant-strength and constant-speed interventions. In particular, abrupt changes in $\gamma(t)$ will not affect the incidence immediately due to delays in isolating individuals. Finally, the instantaneous reproduction number is given by:

$$\mathcal{R}_{\mathrm{i}}(t) = \beta(t)S(t) \int_0^{\infty} \exp\left(-\int_{t-\tau}^{t} \gamma(s)\,\mathrm{d}s\right) \mathrm{d}\tau. \tag{33}$$

When $\gamma(t) = \gamma(0)$, we obtain a familiar form: $\mathcal{R}_{\mathrm{i}}(t) = \mathcal{R}_0 S(t)$, where $\mathcal{R}_0 = \beta(0)/\gamma(0)$.

Here, we compare two different scenarios, in which interventions are introduced and are later partially lifted (Fig. 2). First, we consider a smooth introduction and lifting of

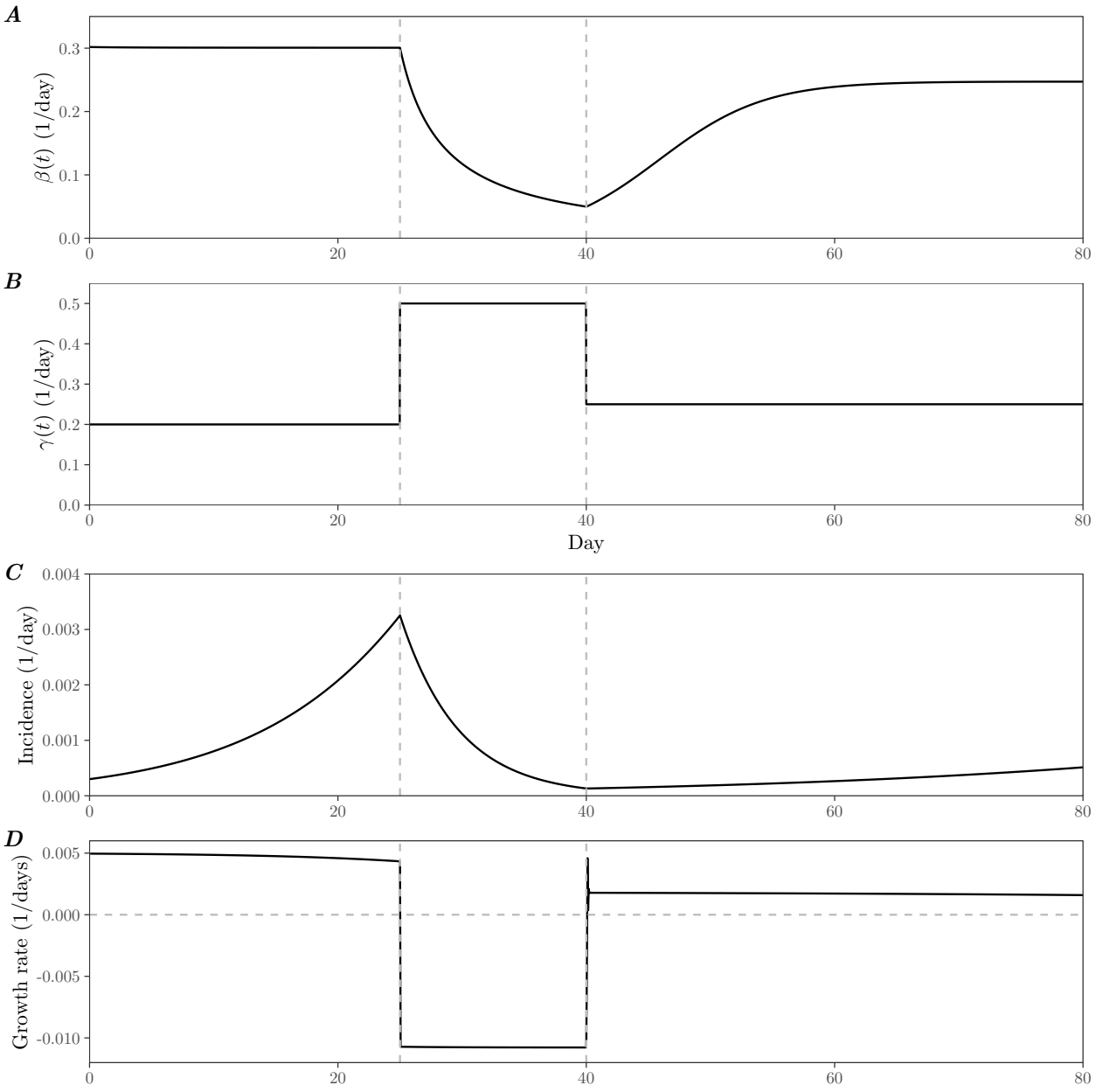

Figure 2: **Assumed changes in transmission and removal rate.** The semi-mechanistic SIR model is simulated under two different scenarios. (A) Equivalent strength-based intervention scenario. Removal rate γ is fixed to 0.2/day throughout. (B) Equivalent speed-based intervention scenario. Transmission rate β is fixed to 0.3/day throughout. (C) Instantaneous incidence under equivalent strength- and speed-based intervention scenarios. (D) Growth rate estimates over time. Equivalent strength- and speed-based scenarios give identical incidence trajectories.

a constant-strength intervention, modeled by changes in β while fixing γ (Fig. 2A). Next,

we consider a sudden introduction and lifting of a constant-speed intervention, modeled by changes in γ while fixing β (Fig. 2B). We refer to these two interventions as *equivalent* constant-strength and constant-speed interventions because they give identical incidence curves (Fig. 2C), demonstrating that changes in β and γ cannot be jointly identified from the incidence curve alone (see Methods and Materials). In both cases, growth rate $r(t)$ estimates are identical (Fig. 2D); as we show later, however, changes in reproduction numbers differ between the two scenarios.

Epidemiological dynamics under a constant-strength intervention are presented in Fig. 3. In this case, the proportional reproduction number $\mathcal{R}_{\text{cori}}(t)$, which relies on the intrinsic generation-interval distribution, matches the instantaneous reproduction number $\mathcal{R}_{\text{i}}(t)$, which relies on the instantaneous generation-interval distribution (Fig. 3A). Therefore, we are able to correctly estimate $\mathcal{R}_{\text{i}}(t)$ using `EpiEstim` (Fig. 3A). The initial overestimation from `EpiEstim` is caused by the left censoring (Gostic et al., 2020). Minor differences between `EpiEstim` estimates and $\mathcal{R}_{\text{cori}}(t)$ are caused by discretization.

Likewise, we can accurately estimate the case reproduction number $\mathcal{R}_{\text{c}}(t)$ using the classic Wallinga-Teunis estimator (based on the intrinsic generation-interval distribution) (Fig. 3B). This is because the instantaneous generation-interval distribution does not change over time under constant-strength interventions (Fig. 3C). Using the forward generation-interval distribution, instead of the instantaneous generation-interval distribution, matches neither $\mathcal{R}_{\text{i}}(t)$ ($\mathcal{R}_{\text{forward}}(t)$ in Fig. 3A) nor $\mathcal{R}_{\text{c}}(t)$ in this case ($\mathcal{R}_{\text{forward}}(t)$ in Fig. 3B) because the forward distribution changes, even when the instantaneous distribution does not change (Fig. 3C). As described earlier (Fig. 1A–C), introducing and lifting a constant-strength intervention cause the forward generation intervals become shorter and longer, respectively (Fig. 3C). The backward distribution exaggerates these changes through the epidemic growth/decay effect—when an epidemic is growing (decaying), the mean backward intervals become shorter (longer).

Epidemiological dynamics under a constant-speed intervention are presented in Fig. 4. In this case, the instantaneous generation-interval distribution changes through time. $\mathcal{R}_{\text{cori}}(t)$ differs from the true $\mathcal{R}_{\text{i}}(t)$ (Fig. 4A) because the constant-speed interventions lead to changes in the instantaneous generation-interval distribution (Fig. 4C). Therefore, `EpiEstim` inaccurately estimates $\mathcal{R}_{\text{i}}(t)$ (Fig. 4A)— in particular, `EpiEstim` estimates that $\mathcal{R}_{\text{i}}(t)$ crossed the threshold $\mathcal{R}_{\text{i}}(t) = 1$ later (around $t = 55$) than it actually did (around $t = 45$).

Using the intrinsic distribution is also problematic for estimating the case reproduction number $\mathcal{R}_{\text{c}}(t)$ (Fig. 4B). The true $\mathcal{R}_{\text{c}}(t)$ changes sharply, reflecting sharp changes in the removal rate $\gamma(t)$ (Fig. 2B), but using the intrinsic distribution gives smooth estimates of $\mathcal{R}_{\text{c}}(t)$. In this case, $\mathcal{R}_{\text{forward}}(t)$ matches $\mathcal{R}_{\text{i}}(t)$ and $\mathcal{R}_{\text{c}}(t)$ better than their corresponding estimates using the intrinsic generation-interval distribution (EpiEstim and Wallinga-Teunis in Fig. 4, respectively) because the forward generation-interval distribution captures the effects of the constant-speed intervention (Fig. 4C). Surprisingly, the backward generation-interval distribution stays nearly constant because the effect of decreasing incidence (which lengthens the backward generation intervals) cancels out with that of shorter realized generation intervals, caused by the constant-speed intervention (Fig. 4C).

Comparing simulations under equivalent constant-strength and constant-speed interven-

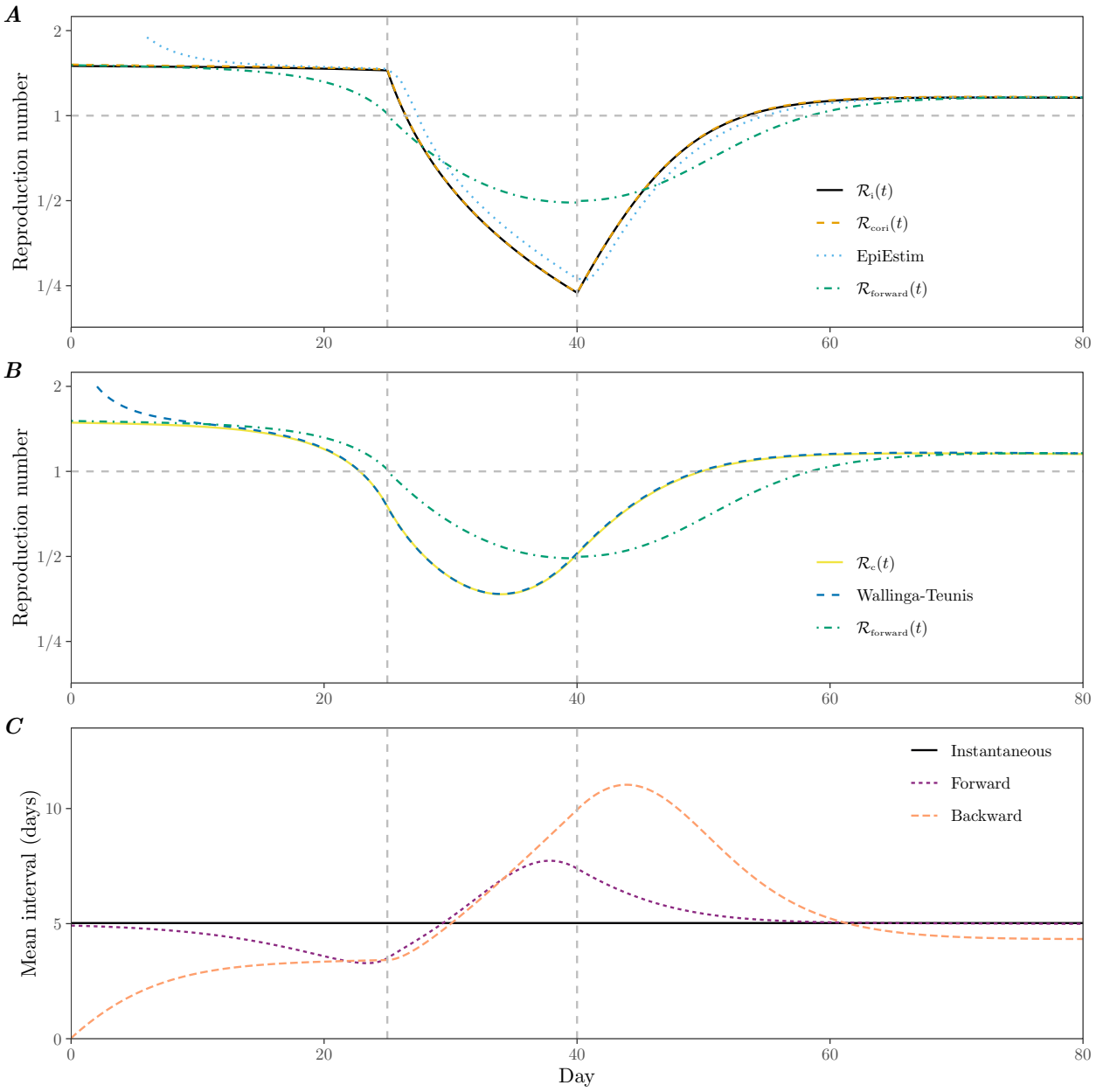

Figure 3: **Epidemiological dynamics of a semi-mechanistic SIR model under equivalent strength-based intervention.** (A) Changes in true instantaneous reproduction number $\mathcal{R}_{\mathrm{i}}(t)$, proportional reproduction number $\mathcal{R}_{\mathrm{cori}}(t)$, estimated $\mathcal{R}_{\mathrm{i}}(t)$ using EpiEstim (assuming a population of one million), and estimated $\mathcal{R}_{\mathrm{forward}}(t)$ using the forward generation-interval distribution. (B) Changes in true case reproduction number $\mathcal{R}_{\mathrm{c}}(t)$, estimated $\mathcal{R}_{\mathrm{c}}(t)$ using Wallinga-Teunis estimator with intrinsic generation-interval distribution, and estimated $\mathcal{R}_{\mathrm{forward}}(t)$ using the forward generation-interval distribution. (C) Changes in mean instantaneous, forward, and backward generation intervals.

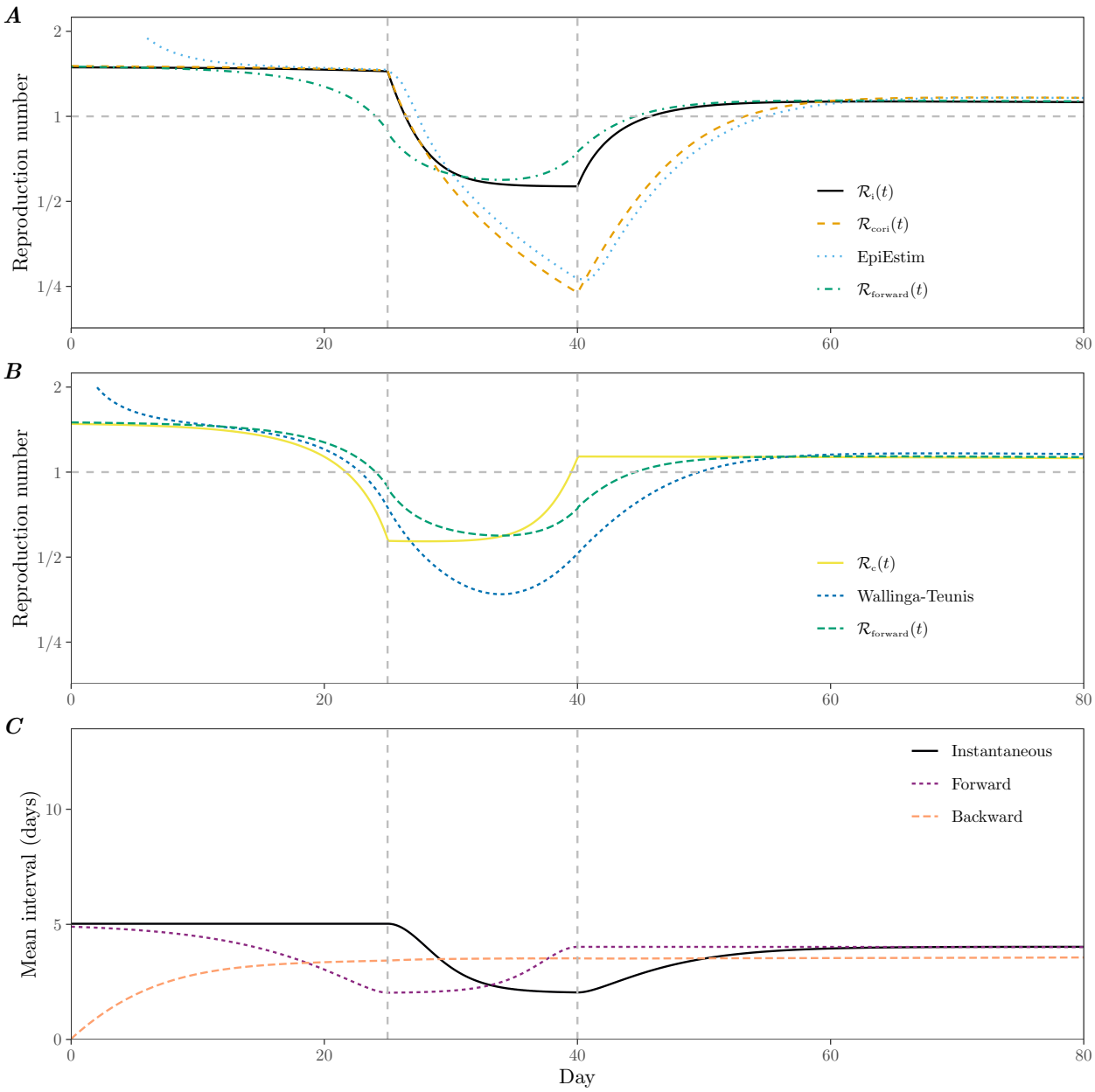

Figure 4: **Epidemiological dynamics of a semi-mechanistic SIR model under equivalent speed-based intervention.** (A) Changes in true instantaneous reproduction number $\mathcal{R}_{\mathrm{i}}(t)$, proportional reproduction number $\mathcal{R}_{\mathrm{cori}}(t)$, estimated $\mathcal{R}_{\mathrm{i}}(t)$ using EpiEstim (assuming a population of one million), and estimated $\mathcal{R}_{\mathrm{forward}}(t)$ using the forward generation-interval distribution. (B) Changes in true case reproduction number $\mathcal{R}_{\mathrm{c}}(t)$, estimated $\mathcal{R}_{\mathrm{c}}(t)$ using Wallinga-Teunis estimator with intrinsic generation-interval distribution, and estimated $\mathcal{R}_{\mathrm{forward}}(t)$ using the forward generation-interval distribution. (C) Changes in mean instantaneous, forward, and backward generation intervals.

tions allows us to better understand the differences between the $\mathcal{R}_{\mathrm{i}}(t)$ and $r(t)$ in capturing current conditions at time t. Under a constant-strength intervention, $\mathcal{R}_{\mathrm{i}}(t) = \beta(t)/\gamma(0)$, and therfore $\mathcal{R}_{\mathrm{i}}(t)$ crosses the threshold, $\mathcal{R}_{\mathrm{i}}(t) = 1$, when $\beta(t)$ crosses the threshold, $\beta(t) = \gamma(0)$ (compare Fig. 2A with Fig. 3A). Under a constant-speed intervention, however, sharp changes in $\gamma(t)$ translate to smooth changes in $\mathcal{R}_{\mathrm{i}}(t)$, and therefore $\mathcal{R}_{\mathrm{i}}(t)$ crosses the threshold, $\mathcal{R}_{\mathrm{i}}(t) = 1$, later (compare Fig. 2B with Fig. 4A). Instead, sharp changes in $\gamma(t)$ are captured by sharp changes in $r(t)$ (compare Fig. 2B with Fig. 2D)—this can readily seen by deriving an explicit expression for $r(t)$:

$$r(t) = \frac{1}{i(t)} \frac{\mathrm{d}i(t)}{\mathrm{d}t} \tag{34}$$

$$= \frac{1}{\beta(t)} \frac{\mathrm{d}\beta(t)}{\mathrm{d}t} - \beta(t)I + \beta(t)S - \gamma(t) \tag{35}$$

where the instantaneous incidence corresponds to $i(t) = \beta(t)SI$ for the semi-mechanistic SIR model. Eq. 35 also shows that changes in $\beta(t)$ is going to have non-trivial effects on $r(t)$, which depend not only on $\beta(t)$ itself but also on per-capita changes in $\beta(t)$ and both state variables, S and I. Therefore, $\mathcal{R}_{\mathrm{i}}(t)$ is the best measure for capturing current conditions at time t under constant-strength interventions, whereas $r(t)$ is the best measure for capturing current conditions at time t under constant-speed interventions.

4 Discussion

The impact of epidemic interventions are often characterized by changes in "effective" reproduction numbers, $\mathcal{R}(t)$. Despite historical emphasis on estimating $\mathcal{R}(t)$, current frameworks neglect possibility that the underlying generation-interval distribution can change over time—an insight that goes back > 10 years (Fraser, 2007). Here, we distinguish two reproduction numbers—instantaneous reproduction number $\mathcal{R}_{\mathrm{i}}(t)$ and case reproduction number $\mathcal{R}_{\mathrm{c}}(t)$, which describe counterfactual and realized transmission processes, respectively—and show that both reproduction numbers can correctly describe the renewal process of infection when paired with correct generation-interval distributions. In particular, a counterfactual generation-interval distribution, which we refer to as the instantaneous generation-interval distribution, is required to correctly estimate the instantaneous reproduction number. This distribution is affected by constant-speed, but not constant-strength, interventions. Neglecting changes in this distribution gives biased estimates of $\mathcal{R}_{\mathrm{i}}(t)$, including estimates of when $\mathcal{R}_{\mathrm{i}}(t)$ crosses the threshold value of 1. Instead, time-dependent growth rate $r(t)$ is a better measure for characterizing the impact of epidemic intervention under a constant-speed intervention.

In practice, estimating the instantaneous generation-interval distribution is expected to be difficult as it systematically differs from the realized generation intervals: even if we can observe all realized generation intervals throughout an epidemic, estimating the instantaneous distribution $g(t, \tau)$ is not trivial. For example, even within a homogeneously mixing population, in which the disease is allowed to spread unchecked (and therefore $g(t, \tau) = g_0(\tau)$

for all t), aggregating all realized generation intervals underestimates the mean intrinsic generation interval due to susceptible depletion (Park et al., 2020). Novel statistical methods are needed to accurately estimate the instantaneous distribution $g(t, \tau)$.

Most state-of-art statistical softwares for estimating reproduction numbers assume that the instantaneous generation-interval distribution does not change across time (e.g., (Abbott et al., 2020; Flaxman et al., 2020; Brauner et al., 2021)). We refer to these estimates as proportional reproduction number $\mathcal{R}_{\text{cori}}$ as they capture proportional reduction in incidence, rather than transmission. While this may be the most parsimonious and best available approach for estimating $\mathcal{R}(t)$, we encourage researchers to not overemphasize the value of this reproduction number estimate, especially whether it crosses the threshold value or not—in particular, this reproduction number estimate can differ systematically from the true instantaneous reproduction number $\mathcal{R}_{\text{i}}$ under speed-like interventions such as contact tracing. Emergence of new variants with a different infectiousness profile (and therefore the intrinsic generation-interval distribution) is expected to have similar effects.

In the context of the current SARS-CoV-2 pandemic, assuming a time-invariant generation-interval distribution could have been justified during the early period given that most interventions were strength-like, including lockdowns, school closures, and travel bans (Flaxman et al., 2020; Li et al., 2021; Brauner et al., 2021). Nonetheless, speed-like interventions, including intense contact tracing efforts (Park et al., 2020) and introduction of contact tracing apps (Wymant et al., 2021), had clear, non-negligible impact on the overall spread; these interventions, including awareness-driven behavioral changes (which can cause symptomatic individuals to self-isolate faster), are likely to have shortened the instantaneous generation intervals by preventing transmission during later stages of infection. Therefore, current estimates of $\mathcal{R}_{\text{i}}$ which relies on early estimates of the generation-interval distributions may be biased and reassessed. Future studies should also consider incorporating hazard-based changes for modeling speed-like interventions.

The renewal equation framework based on the instantaneous form (Eq. 3) has been widely used in epidemic modeling due to its flexibility. A few studies relied on the forward form (Eq. 5), but they incorrectly assumed a time-invariant generation-interval distribution (Nishiura, 2007; Alvarez et al., 2020; White et al., 2021). As we show here, the forward generation-interval distributions, which change over time as transmission conditions change, correctly links the renewal process when paired with the case reproduction number. To our knowledge, this is the first study to correctly link the case reproduction number with the forward renewal equation and to demonstrate the equivalence between the forward and instantaneous renewal formulations— even when the case reproduction number was first introduced by Wallinga and Teunis (2004), they did not explicitly link the case reproduction number to the renewal process. Our study provides theoretical foundation for modeling epidemic processes.

[**SWP:** *Jonathan, can you try writing the last paragraph of the discussion?*]

5 Methods

5.1 Equivalent strength- and speed-based interventions

Here, we model a simple scenario in which a flu-like pathogen with $\mathcal{R}_0 = 1.5$ invades an immunologically naive population using the semi-mechanistic SIR model (Eq. 29–Eq. 31). We begin by modeling speed-based intervention and find the equivalent strength-based intervention. In particular, we assume that the disease spreads without any intervention in the beginning; on day 25, an intense case isolation measure is implemented; and on day 40, the intervention is partially lifted. This is modeled as follows:

$$\beta(t) = 3/10 \text{ days}^{-1}, \gamma(t) = \begin{cases} 1/5 \text{ days}^{-1} & t < 25 \\ 1/2 \text{ days}^{-1} & 25 \leq t < 40 \\ 1/4 \text{ days}^{-1} & 40 \leq t \end{cases}. \tag{36}$$

Simulations are run for 100 days based on the following initial conditions: $S(0) = 1 - 10^{-3}$, $I(0) = 10^{-3}$, and $R(0) = 0$.

Since we assume that incidence is known exactly until time t^*, we can, in fact, estimate the transmission rate $\beta^*(t)$ (with fixed $\gamma(t) = \gamma(0)$) that gives identical incidence trajectory until time t^*. This transmission rate is given by:

$$\beta^*(t) = \frac{\mathcal{R}_{\text{cori}}(t)\gamma(0)}{S(t)}, \tag{37}$$

where the proportional reproduction number $\mathcal{R}_{\text{cori}}$ is calculated from the incidence curve $i(t)$. More generally, given true incidence $i(t)$ until time t^*, modulated by any combination of strength- and speed-based interventions, we can find equivalent strength-based intervention $\mathcal{P}^*(t)$ until time t^*:

$$\mathcal{P}^*(t) = \frac{\mathcal{R}_{\text{cori}}(t)}{\mathcal{R}_0 S(t)}, \tag{38}$$

which generates an identical incidence curve when the initial conditions are identical.

References

Abbott, S., J. Hellewell, R. Thompson, K. Sherratt, H. Gibbs, N. Bosse, J. Munday, S. Meakin, E. Doughty, J. Chun, Y. Chan, F. Finger, P. Campbell, A. Endo, C. Pearson, A. Gimma, T. Russell, n. null, S. Flasche, A. Kucharski, R. Eggo, and S. Funk (2020). Estimating the time-varying reproduction number of SARS-CoV-2 using national and subnational case counts [version 2; peer review: 1 approved with reservations]. *Wellcome Open Research 5*(112).

Aldis, G. and M. Roberts (2005). An integral equation model for the control of a smallpox outbreak. *Mathematical biosciences 195*(1), 1–22.

Ali, S. T., L. Wang, E. H. Lau, X.-K. Xu, Z. Du, Y. Wu, G. M. Leung, and B. J. Cowling (2020). Serial interval of SARS-CoV-2 was shortened over time by nonpharmaceutical interventions. *Science 369*(6507), 1106–1109.

Alvarez, L., M. Colom, and J.-M. Morel (2020). A variational model for computing the effective reproduction number of sars-cov-2. *medRxiv*.

Anderson, R. M. and R. M. May (1991). *Infectious diseases of humans: dynamics and control*. Oxford university press.

Brauner, J. M., S. Mindermann, M. Sharma, D. Johnston, J. Salvatier, T. Gavenčiak, A. B. Stephenson, G. Leech, G. Altman, V. Mikulik, et al. (2021). Inferring the effectiveness of government interventions against COVID-19. *Science 371*(6531).

Champredon, D. and J. Dushoff (2015). Intrinsic and realized generation intervals in infectious-disease transmission. *Proceedings of the Royal Society B: Biological Sciences 282*(1821), 20152026.

Champredon, D., J. Dushoff, and D. J. D. Earn (2018). Equivalence of the Erlang-distributed SEIR epidemic model and the renewal equation. *SIAM Journal on Applied Mathematics 78*(6), 3258–3278.

Cori, A., N. M. Ferguson, C. Fraser, and S. Cauchemez (2013). A new framework and software to estimate time-varying reproduction numbers during epidemics. *American journal of epidemiology 178*(9), 1505–1512.

Diekmann, O. and J. A. P. Heesterbeek (2000). *Mathematical epidemiology of infectious diseases: model building, analysis and interpretation*, Volume 5. John Wiley & Sons.

Diekmann, O., J. A. P. Heesterbeek, and J. A. Metz (1990). On the definition and the computation of the basic reproduction ratio $\mathcal{R}_0$ in models for infectious diseases in heterogeneous populations. *Journal of mathematical biology 28*(4), 365–382.

Dushoff, J. and S. W. Park (2021). Speed and strength of an epidemic intervention. *Proceedings of the Royal Society B 288*(1947), 20201556.

Flaxman, S., S. Mishra, A. Gandy, H. J. T. Unwin, T. A. Mellan, H. Coupland, C. Whittaker, H. Zhu, T. Berah, J. W. Eaton, et al. (2020). Estimating the effects of non-pharmaceutical interventions on COVID-19 in europe. *Nature 584*(7820), 257–261.

Fraser, C. (2007). Estimating individual and household reproduction numbers in an emerging epidemic. *PloS one 2*(8), e758.

Gostic, K. M., L. McGough, E. B. Baskerville, S. Abbott, K. Joshi, C. Tedijanto, R. Kahn, R. Niehus, J. A. Hay, P. M. De Salazar, et al. (2020). Practical considerations for measuring the effective reproductive number, R_t. *PLoS computational biology 16*(12), e1008409.

Heesterbeek, J. and K. Dietz (1996). The concept of $\mathcal{R}_0$ in epidemic theory. *Statistica Neerlandica 50*(1), 89–110.

Kenah, E., M. Lipsitch, and J. M. Robins (2008). Generation interval contraction and epidemic data analysis. *Mathematical biosciences 213*(1), 71–79.

Li, Y., H. Campbell, D. Kulkarni, A. Harpur, M. Nundy, X. Wang, H. Nair, U. N. for COVID, et al. (2021). The temporal association of introducing and lifting non-pharmaceutical interventions with the time-varying reproduction number (R) of SARS-CoV-2: a modelling study across 131 countries. *The Lancet Infectious Diseases 21*(2), 193–202.

Liu, Q.-H., M. Ajelli, A. Aleta, S. Merler, Y. Moreno, and A. Vespignani (2018). Measurability of the epidemic reproduction number in data-driven contact networks. *Proceedings of the National Academy of Sciences 115*(50), 12680–12685.

Nishiura, H. (2007). Time variations in the transmissibility of pandemic influenza in Prussia, Germany, from 1918–19. *Theoretical Biology and Medical Modelling 4*(1), 1–9.

Nishiura, H. (2010). Time variations in the generation time of an infectious disease: implications for sampling to appropriately quantify transmission potential. *Mathematical Biosciences & Engineering 7*(4), 851.

Pan, A., L. Liu, C. Wang, H. Guo, X. Hao, Q. Wang, J. Huang, N. He, H. Yu, X. Lin, et al. (2020). Association of public health interventions with the epidemiology of the COVID-19 outbreak in Wuhan, China. *Jama 323*(19), 1915–1923.

Parag, K. V., R. N. Thompson, and C. A. Donnelly. Are epidemic growth rates more informative than reproduction numbers? *Journal of the Royal Statistical Society: Series A (Statistics in Society) n/a*(n/a).

Park, S. W., D. Champredon, and J. Dushoff (2020). Inferring generation-interval distributions from contact-tracing data. *Journal of the Royal Society Interface 17*(167), 20190719.

Park, S. W., K. Sun, D. Champredon, M. Li, B. M. Bolker, D. J. Earn, J. S. Weitz, B. T. Grenfell, and J. Dushoff (2020). Forward-looking serial intervals correctly link epidemic growth to reproduction numbers. *Proceedings of the National Academy of Sciences 118*(2).

Park, Y. J., Y. J. Choe, O. Park, S. Y. Park, Y.-M. Kim, J. Kim, S. Kweon, Y. Woo, J. Gwack, S. S. Kim, et al. (2020). Contact tracing during coronavirus disease outbreak, South Korea, 2020. *Emerging infectious diseases 26*(10), 2465–2468.

Roberts, M. (2004). Modelling strategies for minimizing the impact of an imported exotic infection. *Proceedings of the Royal Society of London. Series B: Biological Sciences 271*(1555), 2411–2415.

Roberts, M. and J. Heesterbeek (2007). Model-consistent estimation of the basic reproduction number from the incidence of an emerging infection. *Journal of mathematical biology 55*(5-6), 803.

Svensson, Å. (2007). A note on generation times in epidemic models. *Mathematical biosciences 208*(1), 300–311.

Wallinga, J. and P. Teunis (2004). Different epidemic curves for severe acute respiratory syndrome reveal similar impacts of control measures. *American Journal of epidemiology 160*(6), 509–516.

White, L. F., C. B. Moser, R. N. Thompson, and M. Pagano (2021). Statistical estimation of the reproductive number from case notification data. *American Journal of Epidemiology 190*(4), 611–620.

Wymant, C., L. Ferretti, D. Tsallis, M. Charalambides, L. Abeler-Dörner, D. Bonsall, R. Hinch, M. Kendall, L. Milsom, M. Ayres, C. Holmes, M. Briers, and C. Fraser (2021). The epidemiological impact of the NHS COVID-19 App. *Nature*.